

## Asian Journal of Scientific Research

ISSN 1992-1454





ISSN 1992-1454 DOI: 10.3923/ajsr.2017.43.49



### **Research Article**

# Deposition and Characterization of Nickel Selenide Thin Films for Applications in Optoelectronic Devices

<sup>1</sup>P.A. Nwofe, <sup>2</sup>R.A. Chikwenze, <sup>1</sup>P.E. Agbo and <sup>1</sup>H.U. Igwe

<sup>1</sup>Division of Materials Science and Renewable Energy, Department of Industrial Physics, Ebonyi State University, Abakaliki, Nigeria <sup>2</sup>Department of Physics, Faculty of Science and Technology, Federal University, Ndufu-Alike, Ikwo, Nigeria

#### **Abstract**

**Objective:** This study is a fundamental step towards achieving the optimized conditions needed to improve efficiencies of NiSe-based solar cell devices. **Methodology:** Thin films of NiSe (nickel selenide) were deposited at different concentrations (0.10-1.00 M) using the chemical bath deposition technique. The other deposition variables were kept constant. The films were characterized using optical spectroscopy to investigate the absorbance, transmittance and reflectance versus wavelength measurements. **Results:** The results show that the absorbance of the films were very low (<1%), indicating that the films were highly transmitting (>50%). The optical absorption coefficient were >10<sup>4</sup> cm<sup>-1</sup>, the energy bandgap was direct with values in the range 1.60-2.0 eV. **Conclusion:** These values strongly suggest the use of these films in device fabrication especially in solar cell devices.

Key words: Concentration, energy bandgap, optical spectroscopy, optical absorption coefficient, solar cells

Received: March 21, 2016 Accepted: July 24, 2016 Published: December 15, 2016

Citation: P.A. Nwofe, R.A. Chikwenze, P.E. Agbo and H.U. Igwe, 2017. Deposition and characterization of nickel selenide thin films for applications in optoelectronic devices. Asian J. Sci. Res., 10: 43-49.

Corresponding Author: P.A. Nwofe, Division of Materials Science and Renewable Energy, Department of Industrial Physics, Ebonyi State University, Abakaliki, Nigeria

Copyright: © 2017 P.A. Nwofe *et al.* This is an open access article distributed under the terms of the creative commons attribution License, which permits unrestricted use, distribution and reproduction in any medium, provided the original author and source are credited.

Competing Interest: The authors have declared that no competing interest exists.

Data Availability: All relevant data are within the paper and its supporting information files.

#### **INTRODUCTION**

In recent times, thin films of metal chalcogenides (selenides, sulphides and tellurides) are currently gaining more interest for applications in various electronic, optoelectronics, nanotechnology and in photonic devices. This because of their tunable properties and ease of fabrication. Nickel selenides has been widely used in different devices including solar cells, photoconductors, coatings and IR detectors<sup>1-6</sup>. Thin film surface coating are mostly used for efficient conversion of solar radiation into many useful applications. Nickel pigmented aluminum oxide on aluminum is also gaining prominence in the markets because it exhibit advantageous properties like; high tensile strength, low density and corrosion resistance at high temperatures. In the literature, it has been reported that NiSe thin films can be grown using low cost deposition methods including chemical bath deposition<sup>4-7</sup>, electro-deposition<sup>2,3,8-12</sup>, nano-wire arrays<sup>13</sup>, solvothermal synthesis 14,15, hydrothermal synthesis 16-18 and chemical vapour deposition<sup>19</sup>.

Chemical bath deposition is more widely used in thin film deposition, compared to other deposition techniques because it is cost effective and also produce high quality thin films. Reports on nickel selenides thin films grown by different methods are relatively rare in the literature hence, the major aim of the present investigation are: (i) To grow thin films of nickel selenides by using a low cost deposition technique, (ii) To characterize the layers using standard characterization techniques, (iii) Investigate the dependence of the optical properties of the films on different concentrations and (iv) To establish their suitability for applications in optoelectronics and photonic devices. The study reported herein is a fundamental step towards improving the properties of nickel selenide thin films hence the dependence of the optical properties on the deposition variable (concentration) are presented.

#### **MATERIALS AND METHODS**

Substrate cleaning plays a significant role in thin film deposition. The soda-lime glasses used as substrates were thoroughly cleaned in an ultrasonic bath and then dried. The solution growth of the NiSe involved measuring with syringes, desired volumes of definite molar solutions of the required chemicals for a particular selenide compound to form the growth mixture. The growth mixtures were topped with the growth matrix (water or PVA or PVP) and stirred with magnetic stirrer. In particular, the reaction baths for the deposition of the NiSe thin films contains 5 mL, 1 M

NiCl<sub>2</sub>+10 mL, 25% NH<sub>3</sub>+8 mL, 1 M Na<sub>2</sub>SeSO<sub>3</sub>+40 mL of the growth matrix put in that order into 80 mL beaker. The pH of the reaction bath was in the alkaline range (10.0). The pre-cleaned glass substrates were then inserted into the growth mixtures and held vertically with synthetic foam. The disposition time was fixed for 4 h at a constant temperature of  $60^{\circ}$ C. The films were removed, rinsed with distilled water and then dried in air.

The films were characterized using optical spectroscopy to investigate the transmittance, absorbance and reflectance versus wavelength measurements. The optical characterisation was done with a Unico-UV-2102PC spectrophotometer and the wavelength range was between 300-1100 nm. The data extracted from the transmittance and reflectance measurements were then used to deduce the optical constants.

#### **RESULTS AND DISCUSSION**

Physical observations of the films indicate that the films were whitish in colour and changed relatively milky at the higher concentrations. Figure 1 gives the variation of the absorbance with wavelength in the range 300-1100 nm. The absorbance were higher at the lower wavelengths and decreased with increasing wavelengths. Such behaviour is generally observed in the variation of absorbance with wavelengths in most chalcogenides thin films as reported by various researchers in the literature<sup>4,5</sup>. However, that absorbance were higher for films grown at the concentration >0.25 M. This was attributed to better crystal ordering of the films grown at the higher concentrations.

Figure 2 gives the variation of the transmittance with wavelength in the range 300-1100 nm. As indicated in Fig. 2, the transmittance of the films were very high, indicating that

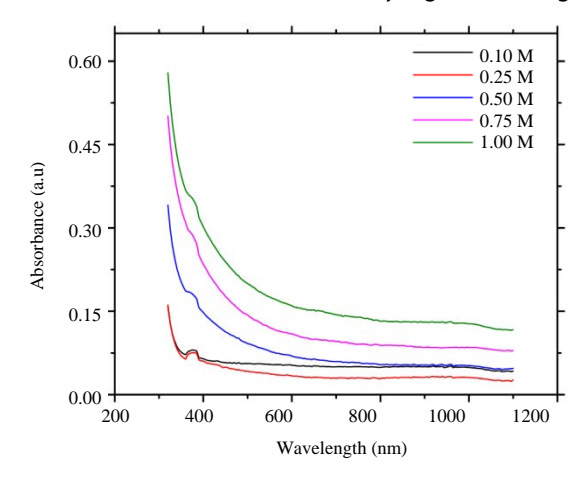


Fig. 1: Plots of absorbance vs wavelength

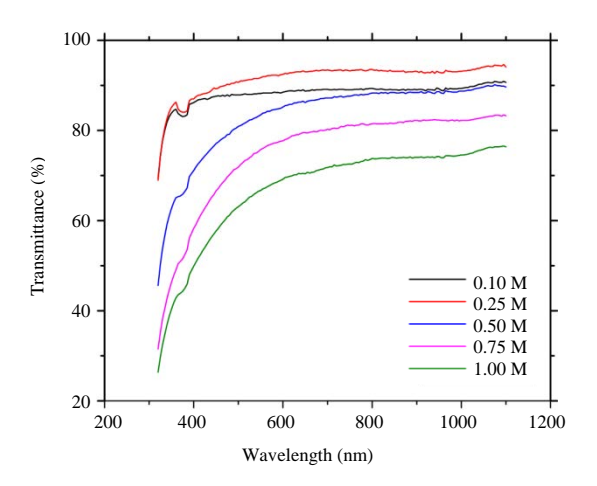


Fig. 2: Plots of transmittance vs wavelength

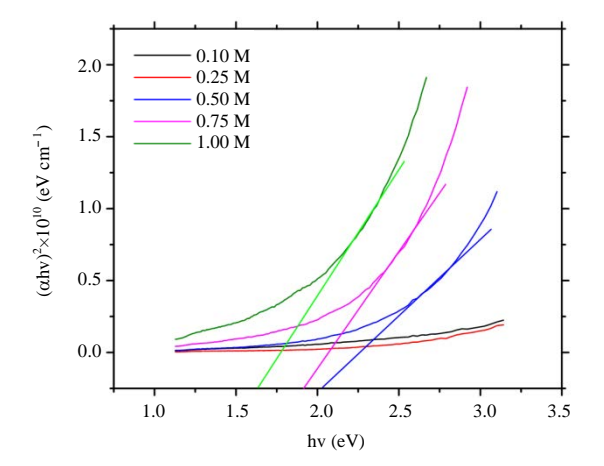


Fig. 3: Plots of  $(\alpha hv)^2$  vs hv

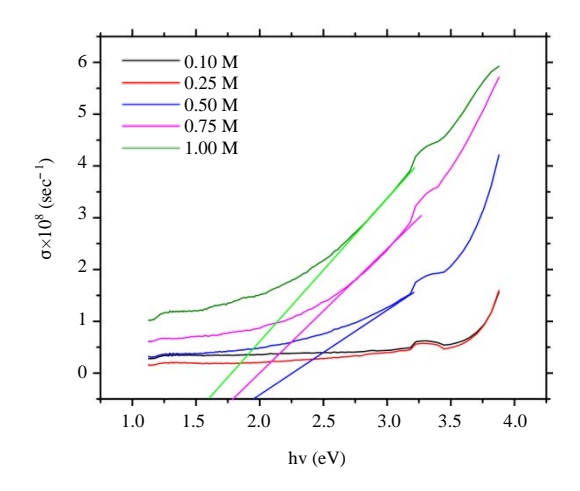


Fig. 4: Plots of optical conductivity vs photon energy

the films can be used in various photonic applications. The data extracted from the absorbance and transmittance

measurements were used to deduce the important optical constants such as the absorption coefficient  $\alpha$ , energy band gap  $E_g$ , extinction coefficients, imaginary dielectric constants, real dielectric constants, dielectric constants and the optical conductivity.

Figure 3 gives typical plots of  $(\alpha hv)^2$  vs hv for the films at the different concentration. The linear portion of the graph of  $(\alpha hv)^2$  vs hv is mostly used to evaluate the energy band gap. The fundamental absorption, which corresponds to an electron excitation from the valence band to the conduction band can be used to determine the nature and value of the optical energy band gap from the plots of  $(\alpha hv)^2$  vs hv, hence extrapolating the linear portion of the graph of  $(\alpha hv)^2$  vs hv gives the value and nature of the energy bandgap.

The energy band gap was calculated using appropriate equations from the literature<sup>20-25</sup>, given as:

$$\alpha h v = B(h v - E_{\varrho})^{n} \tag{1}$$

In Eq. 1, B is an energy independent constant and n is an index that characterizes the optical absorption process. In general, n=0.5 for direct allowed transition and 1.5 for direct forbidden transitions<sup>20</sup>. As indicated in Fig. 3, extrapolation of the linear portion gives energy band gap in the range 1.60-2.0 eV. These values are in agreement with the reports of other research groups<sup>1-5</sup>.

Figure 4 gives typical plots of the variation of the optical conductivity of the films with photon energy at the different concentrations. The optical conductivity was deduced using the relation<sup>23</sup>:

$$\sigma = (\alpha nc)(4\pi)^{-1} \tag{2}$$

In Eq. 2,  $\sigma$  is the optical conductivity,  $\alpha$  is the optical absorption coefficient, n is the refractive index and c is the speed of light in vacuum. The energy band gap can be evaluated from the optical conductivity plots. The values of the energy band gap as shown on Fig. 4 is in agreement with the values obtained earlier (Fig. 3). The values of the energy band gap for films grown at concentration ≤0.25 M were not evaluated as the films were either amorphous or belonged to higher phases of nickel selenides such as Ni<sub>2</sub>Se<sub>3</sub>. It has been generally accepted that materials with energy band gap in the range  $\geq 1.20$  and  $\leq 2.0$  eV are suitable for use in solar cells as absorber layers. This strongly suggest that the films can be used in optoelectronic devices since the optical absorption coefficient is high, the energy band gap is direct, with values in the range suitable for optimum solar energy conversion.

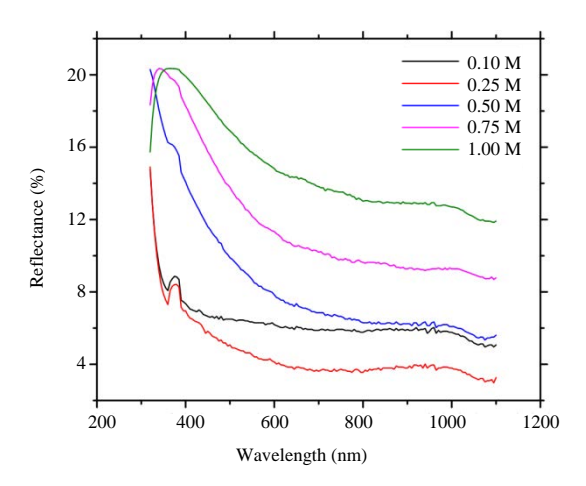


Fig. 5: Plots of reflectance vs wavelength

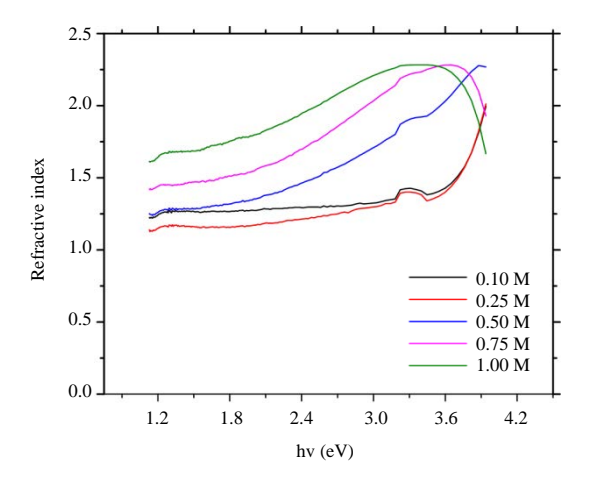


Fig. 6: Plots of refractive index vs photon energy

Figure 5 shows the graph of the reflectance versus wavelength in the range 300-1100 nm. The reflectance were typically low due to the high transmittance values as indicated in Fig. 2. Also the reflectance were higher for films grown at concentration ≥0.50 M and lower for films grown at the lower concentrations. The data extracted from the reflectance plots (Fig. 5) was used to calculate the refractive index using relevant equations from the literature<sup>26-31</sup>. It has been established that the behavior of the thin films in response to incident light is related to its complex refractive index. Accordingly, the equation that relates the refractive index and the reflectance is given as<sup>26</sup>:

$$n = \frac{1 + \sqrt{R}}{1 - \sqrt{R}} \tag{3}$$

In Eq. 3, n is the refractive index and R is the reflectance. Figure 6 gives the variation of the refractive index with the photon energy. The refractive index gives the propagation speed (v) of light in a given material medium according to the relation<sup>20</sup>:

$$n = \frac{c}{v} \tag{4}$$

In Eq. 4, n retains its meanings, c is the speed of light in vacuum and v is the velocity of light in the medium. Equation 4 implies that "n" and "v" are inversely related hence a decrease in "n" means an increase in the velocity "v" at which light propagates in the thin films.

The refractive index were higher at shorter wavelengths (higher photon energy) and lower otherwise. The refractive index was in the range 1.10-2.40. These values are within the range reported by other research groups independent of the deposition techniques<sup>10,32</sup>.

The extinction coefficient is directly related to the optical absorption coefficient and the wavelength under investigation. Accordingly it is given by the relation<sup>33-35</sup>:

$$k = (\alpha \lambda)(4\pi)^{-1} \tag{5}$$

In Eq. 5,  $\alpha$  is the optical absorption coefficient and  $\lambda$  is the wavelength of the incident light. The extinction coefficient decreased in the region of longer wavelength (shorter photon energy) up to a critical wavelength and increased towards shorter wavelength (higher photon energy). This behaviour is usually attributed to the effect free carrier absorption within this region of wavelength. Other authors have reported similar findings in the literature<sup>36-39</sup>.

The complex dielectric constant is related to the refractive index and the extinction coefficient by the relation<sup>20</sup>:

$$\varepsilon = (n + ik)^2 = \varepsilon_i + \varepsilon_r \tag{6}$$

In Eq. 6,  $\epsilon$  is the dielectric constant, n is the refractive index, k is the extinction coefficient,  $\epsilon$  is the complex dielectric constant of the layer,  $\epsilon_i$  and  $\epsilon_r$  are the imaginary and real parts of the dielectric constant. The variation of the extinction coefficient with photon energy is shown on Fig. 7.

Figure 8 shows the variation of the imaginary dielectric constant with photon energy. In Fig. 8, the behaviour is relatively similar to the variation of the extinction coefficient probably due to the relation given in Eq. 6. Figure 9 gives the change in the real dielectric constant with the photon

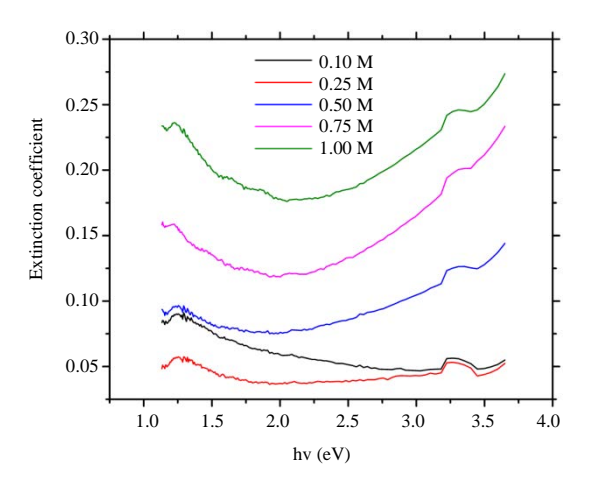


Fig. 7: Plots of extinction coefficient vs photon energy

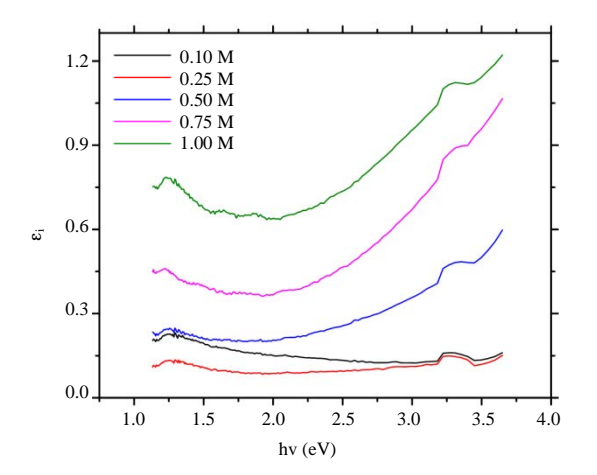


Fig. 8: Plots of imaginary dielectric constant vs photon energy

energies. The real dielectric constant increased with increasing photon energies (shorter wavelength). Other research groups have reported similar behaviour in the literature <sup>36,37</sup>.

Figure 10 show the variation of the dielectric constant with photon energy. In Fig. 10, the behaviour is close to that of the variation of the real dielectric constant with the photon energy (Fig. 9). The films all exhibited a low dielectric constant in the region of longer wavelengths (low energy region). In particular, films grown at concentrations  $\leq 0.25$  M all exhibited very low dielectric constant. The low dielectric constant exhibited in the lower energy region is an indication that devices made with these layers will exhibit relatively low capacitance and hence will display short response time in this wavelength region. In the literature, it has been established that the response time (t) is related to the capacitance (C) and resistance (R) by the equation defined as<sup>40,41</sup>:

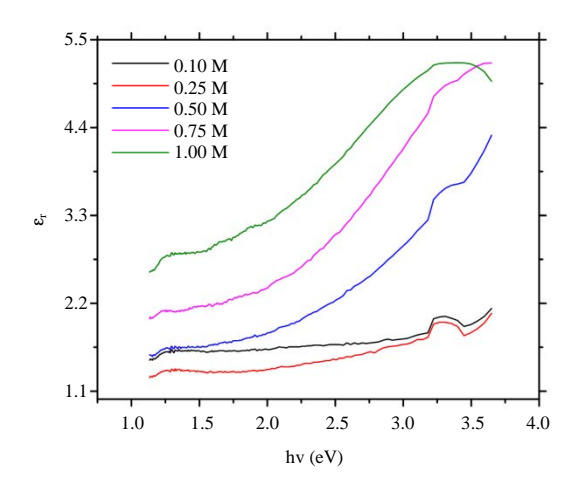


Fig. 9: Plots of real dielectric constant vs photon energy

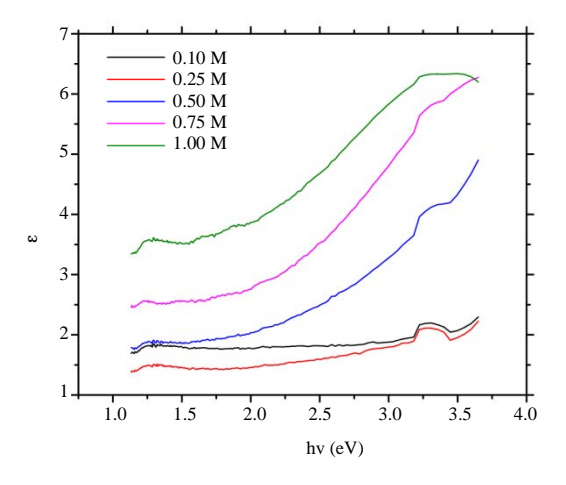


Fig. 10: Plots of dielectric constant vs photon energy

$$t = 2.2RC \tag{7}$$

The low dielectric constant exhibited in the lower energy region clearly indicate that the films could be utilized as fast photodetectors as indicated in Eq. 7.

#### **CONCLUSION**

Thin films of nickel selenides were grown at different concentrations using the chemical bath deposition technique and characterised using optical spectroscopy. The results show that the optical constants varied with the deposition conditions. In particular the energy bandgap of the films grown at concentrations ≥0.50 M were in the range suitable for applications as absorber layer in solar cell devices. The low dielectric constant exhibited by the films especially in the low

energy region and at concentrations  $\le$  0.25 M strongly indicate that the layers can be used in fast photo-detectors. This study is a fundamental step towards achieving the optimized conditions needed to improve efficiencies of NiSe-based solar cell devices and other related optoelectronics devices.

#### **ACKNOWLEDGMENT**

The authors would wish to thank the technical staff of Energy and Materials Research Institute, Akure, Nigeria, for the characterisation of the films.

#### REFERENCES

- Anuar, K., W.T. Tan, A.H. Abdullah, H.M. Jelas, N. Saravanan, S.M. Ho and M. Yazid, 2009. Chemical bath deposition of NiSe thin films from alkaline solutions using triethanolamine as complexing agent. Oriental J. Chem., 25: 813-816.
- 2. Pathak, R.K., P. Wagela, S. Gohar and P. Ramshankar, 2010. Electrochemical preparation and characterization of Ni deposition on aluminum surface. Mater. Sci. Res., 7: 267-272.
- Gohar, S. and R.K. Pathak, 2014. Potentiostatic electrochemical preparation and characterisation of aluminium containing nickel selenide. Orient. J. Chem., 29: 1469-1474.
- Hankare, P.P., B.V. Jadhav, K.M. Garadkar, P.A. Chate, I.S. Mulla and S.D. Delekar, 2010. Synthesis and characterization of nickel selenide thin films deposited by chemical method. J. Alloys Compd., 490: 228-231.
- Hamad, A.H., Z.S. Elmandouch and H.A. Elmeleegi, 2015.
  Structure and some physical properties of chemically deposited Nickel sulfides thin films. Acta Physica Polonia A, 127: 901-903.
- Duan, Y., Q. Tang, B. He, R. Li and L. Yu, 2014. Transparent nickel selenide alloy counter electrodes for bifacial dye-sensitized solar cells exceeding 10% efficiency. Nanoscale, 6: 12601-12608.
- 7. Kassim, A., H.S. Min, T. Tee and Y. Rosli, 2011. Preparation and characterization of chemical bath deposited NiSe thin films. Ozean J. Applied Sci., 4: 363-372.
- 8. Kassim, A., Z. Zainal, S. Nagalingam, D. Kuang and N.H. Sharafaddin, 2004. Electrodeposition of nickel sulfide thin films using triethanolamine as a complexing agent. Chiang Mai J. Sci., 31: 131-137.
- 9. O'Brien, P., J.H. Park and J. Waters, 2003. A single source approach to deposition of nickel sulfide thin films by LP-MOCVD. Thin Solid Films, 431: 502-505.
- Nigam, S., S.K. Patel, S.S. Mahapatra, N. Sharma and K.S. Ghosh, 2015. Nickel coating on high strength low alloy steel by pulse current deposition. IOP Conf. Ser.: Mater. Sci. Eng., Vol. 75.

- 11. Mi, L., Q. Ding, H. Sun, W. Chen and Y. Zhang *et al.*, 2013. One-pot synthesis and the electrochemical properties of nano-structured nickel selenide materials with hierarchical structure. CrystEngComm, 15: 2624-2630.
- Zhang, L., J.C. Yu, M. Mo, L. Wu, Q. Li and K.W. Kwong, 2004. A general solution-phase approach to oriented nanostructured films of metal chalcogenides on metal foils: The case of nickel sulfide. J. Am. Chem. Soc., 126: 8116-8117.
- 13. Lai, C.H., K.W. Huang, J.H. Cheng, C.Y. Lee and W.F. Lee *et al.*, 2009. Oriented growth of large-scale nickel sulfide nanowire arrays via a general solution route for lithium-ion battery cathode applications. J. Mater. Chem., 19: 7277-7283.
- 14. Han, Z.H., S.H. Yu, Y.P. Li, H.Q. Zhao, F.Q. Li, Y. Xie and Y.T.Qian, 1999. Convenient solvothermal synthesis and phase control of nickel selenides with different morphologies. Chem. Mater., 11: 2302-2304.
- 15. Yuan, B., W. Luan and S.T. Tu, 2012. One-step solvothermal synthesis of nickel selenide series: Composition and morphology control. CrystEngComm, 14: 2145-2151.
- Zhuang, Z., Q. Peng, J. Zhuang, X. Wang and Y. Li, 2006. Controlled hydrothermal synthesis and structural characterization of a nickel selenide series. Chem. Eur. J., 12: 211-217.
- Sobhani, A., F. Davar and M. Salavati-Niasari, 2011. Synthesis and characterization of hexagonal nano-sized nickel selenide by simple hydrothermal method assisted by CTAB. Applied Surf. Sci., 257: 7982-7987.
- 18. Sobhani, A., M. Salavati-Niasari and F. Davar, 2012. Shape control of nickel selenides synthesized by a simple hydrothermal reduction process. Polyhedron, 31: 210-216.
- Panneerselvam, A., M.A. Malik, M. Afzaal, P. O'Brien and M. Helliwell, 2008. The chemical vapor deposition of nickel phosphide or selenide thin films from a single precursor. J. Am. Chem. Soc., 130: 2420-2421.
- Pankove, J.I., 1971. Optical Processes in Semiconductors. Courier Corporation, New Jersey, USA., ISBN-13: 9780486602752, Pages: 422.
- 21. Nwofe, P.A., K.R. Reddy, G. Sreedevi, J.K. Tan and R.W. Miles, 2012. Structural, optical and electro-optical properties of thermally evaporated tin sulphide layers. Jpn. J. Applied Phys., Vol. 51. 10.1143/JJAP.51.10NC36
- Nwofe, P.A., R.W. Miles and K.R. Reddy, 2013. Effects of sulphur and air annealing on the properties of thermally evaporated SnS layers for application in thin film solar cell devices. J. Renew. Sustain. Energy, Vol. 5, No. 1. 10.1063/1.4791784
- 23. Nwofe, P.A., K.R. Reddy, J.K. Tan, I. Forbes and R.W. Miles, 2013. On the structural and optical properties of SnS films grown by thermal evaporation method. J. Phys.: Conf. Ser., Vol. 47, No. 1. 10.1088/1742-6596/417/1/012039

- 24. Agbo, P.E., F.U. Nweke, P.A. Nwofe and C.N. Ukwu, 2014. Effects of concentration on the properties of Zn-doped cadmium sulphide thin films. Int. J. Sci. Res., 3: 1832-1837.
- 25. Agbo, P.E., F.U. Nweke, P.A. Nwofe and C.N. Ukwu, 2014. Temperature dependent structural and optical properties of doped cadmium sulphide thin films. Int. J. Adv. Res., 2: 353-358.
- Kumar, K.S., C. Manoharan, S. Dhanapandian and A.G. Manohari, 2013. Effect of Sb dopant on the structural, optical and electrical properties of SnS thin films by spray pyrolysis technique. Spectrochim. Acta Part A: Mol. Biomol. Spectrosc., 115: 840-844.
- 27. Agbo, P.E., P.A. Nwofe and V. Anigbogu, 2015. Synthesis and characterisation of nanocrystalline ZnO-core shell thin films. J. Chem. Biol. Phys. Sci. Sect. C: Phys. Sci., 5: 2926-2929.
- 28. Nwofe, P.A., 2015. Influence of film thickness on the optical properties of antimony sulphide thin films grown by the solution growth technique. Eur. J. Applied Eng. Scient. Res., 4: 1-6.
- 29. Nwofe, P.A., 2015. pH dependent optical properties of chemically deposited  $Sb_2S_3$  thin films. Int. J. Nanomater. Chem., 1: 111-116.
- 30. Nwofe, P.A., 2015. Effect of deposition time on the optical properties of antimony sulphide thin films grown by the solution growth technique. Adv. Applied Sci. Res., 6: 168-173.
- 31. Agbo, P.E. and P.A. Nwofe, 2015. Comprehensive studies on the optical properties of ZnO-Core shell thin films. J. Nanotechnol. Adv. Mater., 3: 63-97.
- 32. Nwofe, P., K.T. Reddy and R.W. Miles, 2013. Influence of deposition time on the properties of highly-oriented SnS thin films prepared using the thermal evaporation method. Adv. Mater. Res., 602-604: 1409-1412.

- 33. Wei, W., L. Mi, Y. Gao, Z. Zheng, W. Chen and X. Guan, 2014. Partial ion-exchange of nickel-sulfide-derived electrodes for high performance supercapacitors. Chem. Mater., 26: 3418-3426.
- 34. Durrani, S.M.A., A.M. Al-Shukri, A. lob and E.E. Khawaja, 2000. Optical constants of zinc sulfide films determined from transmittance measurements. Thin Solid Films, 379: 199-202.
- 35. Nwofe, P.A., K.T.R. Reddy, J.K. Tan, I. Forbes and R.W. Miles, 2012. Thickness dependent optical properties of thermally evaporated SnS thin films. Phys. Procedia, 25: 150-157.
- 36. Mi, L., Y. Chen, W. Wei, W. Chen, H. Hou and Z. Zheng, 2013. Large-scale urchin-like micro/nano-structured NiS: Controlled synthesis, cation exchange and lithium-ion battery applications. RSC Adv., 3: 17431-17439.
- 37. Agbo, P.E. and P.A. Nwofe, 2015. Structural and optical properties of sulphurised  $Ag_2S$  thin films. Int. J. Thin Films Sci. Technol., 4: 9-12.
- 38. Nwofe, P.A. and P.E. Agbo, 2015. Effect of deposition time on the optical properties of cadmium sulphide thin films. Int. J. Thin Films Sci. Technol., 4: 63-67.
- 39. Nwofe, P.A., 2015. Prospects and challenges of silver sulphide thin films: A review. Eur. J. Applied Eng. Sci. Res., 4: 20-27.
- Moloto, N., M.J. Moloto, N.J. Coville and S.S. Ray, 2009.
  Optical and structural characterization of nickel selenide nanoparticles synthesized by simple methods. J. Cryst. Growth, 311: 3924-3932.
- 41. Quimby, R.S., 2006. Photonics and Lasers: An Introduction. John Wiley and Sons, New York, USA., ISBN-13: 9780471791584, Pages: 680.